Published in final edited form as:

Oncogene. 2015 October ; 34(43): 5460–5471. doi:10.1038/onc.2015.1.

Targeting the *hsp70* gene delays mammary tumor initiation and inhibits tumor cell metastasis

Jianlin Gong[1], **Desheng Weng**[1], **Takanori Eguchi**[2], **Ayesha Murshid**[2], **Michael Y. Sherman**[3], **Baizheng Song**[1], **Stuart K. Calderwood**[2]

[1]Department of Medicine, Boston University Medical Center, Boston, MA 02118, USA

[2]Molecular and Cellular Radiation Oncology, Beth Israel Deaconess Medical Center, Harvard Medical School, 21-27 Burlington Avenue, Boston, MA 02215, USA

[3]Department of Biochemistry, Boston University Medical Center, Boston, MA 02118, USA

Abstract

Elevated levels of the inducible heat shock protein 70 (Hsp72) have been implicated in mammary tumorigenesis in histological investigations of human breast cancer. We therefore examined the role of Hsp72 in mice, using animals in which the *hsp70* gene was inactivated. We used a spontaneous tumor system with mice expressing the polyomavirus middle T (PyMT) oncogene under control of the mouse mammary tumor virus (MMTV) long terminal repeat (MMT mice). These mice developed spontaneous, metastatic mammary cancer. We then showed Hsp72 to be upregulated in a fraction of mammary cancer initiating cells (CIC) within the MMT tumor cell population. These cells were characterized by elevated surface levels of stem cell markers CD44 and Sca1 and by rapid metastasis. Inactivation of the *hsp70* gene delayed the initiation of mammary tumors. This delay in tumor initiation imposed by loss of *hsp70* was correlated with a decreased pool of CIC. Interestingly, *hsp70* knockout significantly reduced invasion and metastasis by mammary tumor cells and implicated its product Hsp72 in cell migration and formation of secondary neoplasms. Impaired tumorigenesis and metastasis in *hsp70* knockout MMT mice was associated with down-regulation of the *met* gene and reduced activition of the oncogenic c-Met protein. These experiments therefore showed Hsp72 to be involved in the growth and progression of mammary carcinoma and highlighted this protein as a potential target for anti-cancer drug development.

Keywords

Hsp72; PyMT; Mammary Carcinoma and tumor metastasis

Correspondence address: Jianlin Gong, Department of Medicine, Boston University School of Medicine, 650 Albany Street, Boston, Room 309, MA 02118, jgong@bu.edu or Stuart K. Calderwood, Molecular and Cellular Radiation Oncology, Beth Israel Deaconess Medical Center, Harvard Medical School, 21-27 Burlington Avenue, Boston, MA 02215, USA, scalderw@bidmc.harvard.edu.

Conflict of interest

All authors declare no conflict of interest.

Introduction

During transformation, cells have been shown to vault multiple hurdles to escape cell regulation, and even more obstacles to evolve into macrotumors and metastasize to distant tissue sites (1). During these processes, cancer cell populations were shown to encounter stressful conditions and harsh microenvironments (2). To survive in such unfavorable conditions, cancer cells have been shown to upregulate a variety of proteins for cytoprotection, including heat shock proteins (HSPs) (3, 4). HSPs were first shown to be upregulated under stress conditions and have latterly been shown to be co-opted by oncogenic activation (5, 6). Drugs targeting one of these proteins, Hsp90 are currently under investigation in cancer therapy in clinical trials for a number of cancer types (7–10). However, in addition to Hsp90, another HSP family member, Hsp70 has been proposed as a target in cancer (11–13).

At least 12 members of the human Hsp70 family have been isolated, including proteins expressed in the cytoplasm, endoplasmic reticulum (ER) and mitochondria (14–16). Both constitutively expressed family members [such as human heat shock cognate (HSC) 73] and stress-inducible HSPs (human Hsp72) have been observed (16, 17). The current study involved the murine paralog of Hsp72 referred to here also as Hsp72. Hsp72 was shown to be encoded by two highly conserved genes *hsp70.1* and *hsp70.3* arranged tandemly on the mouse genome and could thus be simultaneously inactivated by homologous recombination (18). We have employed mice with combined knockout of *hsp70.1* and *hsp70.3*, that do not express Hsp72, and for simplicity are referred to here as *hsp70*−/−. The most familiar properties of Hsp70 family members involve protein folding homeostasis and they form part of the molecular chaperone family (14, 19). Hsp72 was shown to be regulated at the transcriptional level by heat shock factor 1 (HSF1), a protein also increased in expression in mammary cancer (4, 20). In addition to chaperoning client proteins, Hsp72 was demonstrated to be a powerful inhibitor of apoptosis and might in this way participate in tumorigenesis (21); Hsp72 was shown to promote cell survival through the mediation of molecules such as Akt/PKB and PKC (22). In addition, Hsp72 suppressed replicative senescence by modulating the activity of the oncogenic co-chaperone Bag3 (23). Consistent with these findings, Hsp72 was found to be expressed at relatively high concentrations in many types of cancer and its abundance was correlated with histological grade, the rate of tumor metastasis and a with poor prognosis (6, 24–29). Indeed, high levels of Hsp72 were strongly implicated in tumor metastasis (26, 30). Elevated expression of Hsp72 and 14–3-3, another protein shown to exert a bridge function by regulating the activity of protein kinases and phosphorylases, was significantly correlated with the extent of metastasis in human triple-negative breast cancer, a subtype of invasive breast cancer (25). These proteins could be used to predict metastatic potential of triple-negative breast cancer with high sensitivities and specificities. Overexpression of Hsp72 was also associated with resistance to some cancer chemotherapy drugs (31, 32). These observations therefore suggested the involvement of the *hsp70* gene in tumorigenesis and further, that Hsp72 might be a promising target in cancer therapy.

Mice expressing the polyomavirus middle T (PyMT) oncogene under control of the mouse mammary tumor virus (MMTV) long terminal repeat develop spontaneous mammary

carcinomas with high metastatic rate to lungs (33). Previously, we used mice (MMT) double transgenic for PyMT and human MUC1 to study the seeding cells of lung metastasis and found that expression of human MUC1 did not influence mammary tumorigenesis and disseminated tumor cells (34). In addition, a subpopulation of these spontaneous mammary tumor cells, a population that expressed surface markers CD44 and Sca1 was implicated as a key player in early dissemination and metastasis to the lungs (34). We therefore aimed in the current study to examine the potential role of *hsp70* in tumorigenesis in this system. To determine such a contribution of *hsp70* in MMT mice, we generated *hsp70*-deficient MMT mice (*hsp70*$^{-/-}$MMT). Our experiments showed *hsp70* to be required for robust tumor initiation, dissemination and metastasis in MMT mice.

Results

Hsp70 levels were upregulated in mammary tumor cells expressing CD44 and Sca1

In our previous studies on MMT spontaneous mouse breast cancer, we found that a mammary tumor cell subpopulation expressing surface markers CD44 and Sca1 played significant roles in tumorigenesis and metastasis relatively early in progression (34). CD44 had been shown to be a surface glycoprotein commonly used as a marker for mammary stem cells and Sca-1 to be a GPI-anchored surface protein whose expression identified the tumor initiating population (35, 36). The CD44 and Sca1 positive cells have been referred to as cancer stem cells (CSC). To further characterize the role of *hsp70* gene expression in the properties of this tumor cell subpopulation, cells from the spontaneously derived mammary tumors were first isolated from MMT mice, stained with anti-CD44 and anti-Sca1 mAbs and sorted into CD44/Sca1^{+} and CD44/Sca1^{-} subsets. The sorted tumor cells were then investigated by immunocytochemical staining with mAbs specific for proteins in the *hsp70* gene expression network and then examined under microscopy. As expected, all tumor cells stained positive for Epithelial Specific Antigen (ESA), consonant with their epithelial origins (Figure 1a, right panel and b). Most tumor cells also expressed HSF1, the regulator of *hsp* gene expression, as observed previously in human mammary cancer (Figure 1a, left panel and b) (37). In contrast, Hsp72 protein and the levels of the activated form of HSF1 that is phosphorylated on serine 326 (phospho-HSF1-S326) (38) were significantly elevated in CD44/Sca1^{+} cells compared to the CD44/Sca1^{-} cells, indicating upregulation of the *hsp70* gene expression network (Figure 1a and b). In addition *metastasis associated protein 1* (MTA1), another HSF1 regulated protein (39), was also increased in CD44/Sca1^{+} cells. These findings suggested that pHSF1, Hsp72 and MTA1 could play roles in the tumorigenic and metastatic properties of CD44/Sca1^{+} tumor cells. We further assessed the functional properties of these two cell populations by assessing cell migration. Mammary tumor cells were sorted into CD44/Sca1^{+} and CD44/Sca1^{-} populations, placed on the upper side of a filter in the migration chamber and cultured for up to 12 hours as previously described (40). The numbers of CD44/Sca1^{+} cells passing through the filter were significantly more than those from CD44/Sca1^{-} tumor cells during culture (Figure 1c and d), suggesting differential functional properties of these two cell populations with regard to migrational properties.

To confirm the upregulation of pHSF1 and Hsp72 in CSC, the enriched mammary tumor cell population was next analyzed with anti-HSP and anti-HSF1 antibodies by Western analysis

of cell lysates. Higher levels of Hsp72, Hsp90 and Hsp110 were observed in the CD44/Sca1^{+} enriched cells compared to the control MMT tumor cells (Figure 2a and b). In addition, similar trends were observed for levels of the activated form of HSF1, phospho-HSF1-S326 (pHSF1). pHSF1 levels were increased in the CD44/Sca1^{+} enriched cells, whereas total HSF1 levels were comparable in each of the populations (Figure 2c and d).

Comparison of mammary tumorigenic and metastatic potential in MMT mice in the presence or absence of hsp70

We next examined the role of the HSF1 product Hsp72 in the tumorigenic and metastatic potential of MMT tumor cells. Mice transgenic for PyMT including MMT mice were shown to develop mammary tumors in 100 % of animals (34, 41–43). To assess the role of Hsp72 in the development of primary and metastatic tumors in MMT mice, we next crossed MMT mice with *hsp70* homozygous knockout mice as well as *hsp70* heterozygotes (Supplementary Figure 1a). To determine whether *hsp70* influences tumor initiation and/or progression, mice were arbitrarily stratified into three age groups for purpose of experiment, including: 25 to 40 days (hyperplastic lesion), 45 to 90 days (mammary intraepithelial neoplasms (MIN), a premalignant stage), and 95 to 130 days (malignant stage). From observing whole mount staining preparations, mammary gland trees in MMT mice showed extensive formation of a dilated ductal system with side buds (Figure 3a, upper left panel). Increased “grape-like” solid masses were observed along the ductal system (Figure 3b and c, upper left panels). These solid masses were derived from epithelial cells, as indicated by ESA staining (Figure 3a, b and c, upper right panels). Similar structures appeared in the mammary gland trees of *hsp70*$^{-/-}$MMT mice, albeit to a lesser degree (Figure 3a, b and c, lower panels). Hyperplastic epithelial nodules or tumor masses were observed in MMT mice, to a lesser extent in *hsp70*$^{+/-}$MMT and *hsp70*$^{-/-}$MMT mice in all age groups. The difference in average size of hyperplastic epithelial nodules or tumor masses among the age groups was statistically significant (Figure 3d). Nevertheless, mammary tumors still eventually developed in *hsp70*$^{-/-}$MMT mice. Interestingly, the mammary tumors that did develop in *hsp70*$^{-/-}$MMT mice tended to be single compared with the multiple tumors that often occurred in MMT mice (data not shown). These experiments showed that tumor initiation induced by PyMT was delayed by the abrogation of *hsp70*, suggesting a role for this gene in tumor initiation at the early stages of tumorigenesis in MMT mice. However, *hsp70* seemed dispensable for primary tumor development at more advanced ages, suggesting compensatory mechanisms that may operate at those later stages (Figure 3c and d).

We next investigated the relative levels of viable disseminated tumor cells in the mice using an *in vitro* colony-forming assay to detect cells with proliferative potential within the lung tissues (34). Previous studies have carefully validated this method for detecting mammary tumor cell dissemination to the lung and colonies were shown to arise from metastasizing mammary tumor cells (34). Numerous cell colonies were detected in cells obtained from the lungs of MMT mice and, to a lesser extent in *hsp70*$^{+/-}$MMT mice (Figure 3e). In contrast, the numbers of tumor cell colonies from the lungs of *hsp*70$^{-/-}$MMT mice in all three stratified age groups were significantly reduced (Figure 3e). Consistent with these findings, metastatic tumors were observed in the lungs of MMT and *hsp70*$^{+/-}$MMT, but not in those

of *hsp*70$^{-/-}$MMT mice (Figure 3f and Table 1). Therefore, the *hsp70 gene* appeared to be essential for lung metastasis in PyMT-induced mammary tumors.

hsp70 inactivation reduced the pool of mammary tumor cells with a CD44/Sca1^{+} phenotype

The experiments above showed tumor initiation and tumor cell dissemination to be affected by *hsp70* knockout (Figure 3). Since cells with the CD44/Sca1^{+} surface phenotype were shown to be pivotal for tumor initiation and metastasis in our previous studies of MMT mice (34), we investigated whether *hsp70* inactivation affected the pool of such cells. Mammary tumor cells were isolated from MMT, *hsp70*$^{+/-}$MMT and *hsp70*$^{-/-}$MMT mice and placed in tissue culture. As shown in Figure 4a, the cells from MMT mice grew to confluence within 36 hours. In contrast, the growth of cells from the *hsp70*$^{-/-}$MMT mice in cell culture was reduced. Many of the cells derived from the *hsp70*$^{-/-}$MMT mice also became detached from the culture plates during growth *in vitro*, as observed by microscope. Similar results were observed in cell viability assay (Figure 4b). *hsp70* thus appeared to regulate the proliferation rate of MMT mammary carcinoma cells. In addition, the fraction of cells staining positive for Sca1 was also significantly decreased in tumor cells from *hsp70*$^{-/-}$MMT compared with those from MMT or *hsp70*$^{+/-}$MMT mice (Figure 4c and d). Thus differences in cell proliferation might be related to the reduced fraction of cells with a CSC phenotype, although differences in proliferative potential in the bulk population could have been involved. The fraction of CD44/Sca1^{+} cells decreased from 9.45% in tumor cells to 2.77 in *hsp70*$^{-/-}$MMT mice (Figure 4e and f). These results suggested that *hsp70* might play a role in maintaining the CD44/Sca1^{+} (CSC) pool in mammary populations.

The retardation of growth in mammary tumor cells from *hsp70*$^{-/-}$MMT mice was further confirmed in the transplantation tumor model. Tumor growth was observed in mice inoculated with tumor cells from MMT (7/7) or *hsp70 heterozygote* MMT (5/7) mice (Figure 4g and h). In contrast, tumors were not detected in mice inoculated with tumor cells from *hsp70*$^{-/-}$MMT (0/7) mice.

Differential capacities for cell migration between mammary tumor cells without or with hsp70

We next determined the ability of tumor cells isolated from wild-type MMT or *hsp70*$^{-/-}$MMT mice to undergo migration under *in vitro* conditions. We initially used a wound-healing assay, in which regions of the monolayer were removed prior to incubation permitting migration of cells into the “wound” in the cell sheet. Using this assay we observed that the numbers of cells from *hsp70*$^{-/-}$MMT mice migrating into the scratch area were considerably reduced compared to those from wild type MMT mice (Figure 5a and b). Differential capacity for migration between wild type MMT and *hsp70*$^{-/-}$MMT tumor cells was next investigated using the two-chamber cell migration assay. While cells from MMT mice were capable of active migration as observed at 2, 6 and 12 hr incubation *in vitro* (Figure 5c, upper panel and d) only a few mammary tumor cells from *hsp70*$^{-/-}$MMT mice migrated and penetrated through the filters (Figure 5c, lower panels and d). Thus, the migratory ability of mammary tumor cells from *hsp70*$^{-/-}$MMT mice appeared to be compromised.

Down regulation of the Met oncogene and hepatic growth factor (HGF) expression in tumors from hsp70 deficient MMT mice

We showed earlier that knockout of the *hsp70* gene in MMT mice reduced metastatic rate. Therefore we next examined the relative expression of metastasis-related genes in tumors from MMT and *hsp70*$^{-/-}$MMT mice by using qPCR array profiling. We examined 89 genes including 5 housekeeping genes in 4 mammary tumors (2 tumors from 2 MMT mice and 2 *hsp70*$^{-/-}$MMT mice, respectively). Among the 89 genes, 50 genes were upregulated in *hsp70*$^{-/-}$MMT mice compared with those from MMT mice, and 39 genes were downregulated (Figure 6a). The upregulated genes in tumors from *hsp70*$^{-/-}$MMT mice that were more than 2-fold increase over the tumors from MMT mice were *Mmp11* (8.03-fold), *Chd4* (3.81), *Pnn* (3.51), *Mdm2* (2.59), *Sstr2* (2.58) and *Fxyd5* (2.22) (Fig. 6a, Table 2). Among the down-regulated genes in the tumors from *hsp70*$^{-/-}$MMT mice, which were expressed less than 0.5-fold comparing with those from MMT mice, were *Met* and its ligand *Hgf* (Table 2). The down-regulation of *Met* and *Hgf* in *hsp70*$^{-/-}$MMT mice was further confirmed by qRT-PCR (Fig. 6b), although only the difference of *Met* expression between MMT and *hsp70*$^{-/-}$MMT mice was statistically significant. In addition, both *hsp70.1* and *hsp70.3* were not detected by the qRT-PCR in *hsp70*$^{-/-}$MMT mice, confirming the knockdown of both genes in these mice (Supplementary Figure 1b). Considering the critical role played by c-Met/Hgf in cell proliferation and invasive growth, and the fact that both ligand (Hgf) and receptor c-Met appeared to depend on Hsp72, we next examined the c-Met activity in mammary tumors using immunohistochemical staining (44, 45). c-Met was shown to become activated, on binding Hgf through a process involving phosphorylation on tyrosine residues Y1349 and Y1356. Thus phospho-c-Met levels in tumors potentially reflected the combined outcome of both c-Met and Hgf expression. We therefore assayed for phospho-c-Met in histological sections of MMT tumors with and without Hsp72 expression. Indeed, many cells positive for phosphorylated c-MET (p-Met) were observed in the tumors from MMT mice (Figure 6c, upper panels and d). In contrast, only few cells were detected in the tumors from *hsp70*$^{-/-}$MMT mice that were positive for p-Met (Figure 6c, lower panels and d). The color in the nuclei of Hsp70 null tumor cells after exposure to anti-P-Met antibodies was similar to that in the PBS exposed slide (Supplementary Figure 2), suggesting background staining with hematoxylin. Interestingly, the p-Met positive cells were scattered along the basal membrane or near the vessels, suggesting that they could include cancer stem cells. Therefore to determine whether p-Met positive cells also expressed stem cell surface markers, we carried out double staining. Many mammary tumor cells from MMT mice were stained positive for p-Met, Sca1 or CD44 (Figure 6e, upper left panels). Interestingly many of the p-Met positive cells also expressed Sca1 or CD44 (Figure 6e, upper right panels; double positive cells stain purple). Cells from *hsp70*$^{-/-}$MMT mice were partially positive for Sca1 or CD44, but not for p-Met in either single or double staining (Figure 6e, lower panels). These results supported the notion that knockout of the *hsp70* gene might result in the reduction of cancer stem cell pool and that this process might also involve loss of Hsp70-dependent c-Met expression and activation. Importantly, knockout of *hsp70* appeared to interrupt the genetic program for invasive growth through a pathway that might involve activated c-Met.

Discussion

Our data implicate the *hsp70* gene in the initiation of tumors in MMT mice and in the metastasic spread that occurs in these mice early after tumor initiation. Similar findings were observed in another model for spontaneous mammary cancer- the Her2 mouse, in which *hsp70* targeting led to reduction in tumorigenesis (46). In the Her2 system, *hsp70* inactivation led to a loss of tumor emergence, likely due to oncogene-induced senescence. By contrast, in the MMT model, tumors emerged and the primary effects of *hsp70* knockout involved metastasis (Figure 3). This difference might be related to the fact that senescence was deterred in the MMT system by the PyMT oncogene. However even in this system there was delayed emergence of tumors in the *hsp*70−/− mice suggesting that suppression of senescence might be incomplete (Figure 3). PyMT has been shown to be a potent oncogene affecting the entire mammary tree, resulting in widespread transformation of the mammary epithelia and rapid production of multifocal mammary adenocarcinomas in 100% of female mice (33, 42, 47). It appeared likely that such synchronized and widespread formation of mammary tumors involved a population of tumor initiating cells. In our previous studies, we showed that tumor cells expressing elevated levels of CD44 and Sca1 possessed tumor initiating capacity and were expressed early in tumorigenesis leading to rapid metastasis (34). Transplantation of the CD44/Sca1^{+} cells from MMT mice into WT mice resulted in the formation of tumors while CD44/Sca1^{-} cells did not seed tumors. These findings suggested the CD44/Sca1^{+} fraction to be a key population of MMT tumor initiating cells. In the present study, we observed elevated Hsp72 levels in CD44/Sca1^{+} cells and impairment of MMT tumorigenesis when the *hsp70* gene was inactivated, indicating a significant role for the chaperone in the functions of these cells. As we showed earlier, the CD44/Sca1^{+} cell population played a key role in metastasis in spontaneous mammary tumors. *Hsp70* may thus have been required for the generation of and / or survival of the CD44/Sca1^{+} cell population. This effect might involve the participation of *Hsp70* in mammary tumor cell proliferation shown in Figure 4A and B. The mechanisms behind *Hsp70* mediated proliferation are not clear although Hsp72 has been found to bind the highly pleiotropic Bag-1 and Bag-3 co-chaperones that may couple Hsp72 expression to cancer / stem cell signaling pathways involved in proliferation (3). However, our findings of downregulated gene expression of the *hgf* and *met* genes and reduced activity of c-Met in *hsp70*$^{-/-}$MMT mice may have provided one potential answer to the mechanisms underlying less robust growth of Hsp72 deficient tumor cells (Table 2 and Figure 6). c-Met was shown to be a proto-oncogene encoding a hepatocyte growth factor receptor and c-Met activity was shown to trigger several downstream pathways including the MAPK cascade, the PI3K-Akt axis, the STAT pathway and the IκBα-NF-κB complex key for cell proliferation and survival (48).

The *hsp70* gene appeared to be required for efficient dissemination of cells from primary mammary tumors. Hsp72 has also been shown to possess the potential to regulate multiple factors involved in mammary tumor cell metastasis in addition to c-Met. Teng Y et al (49) demonstrated that Hsp72 bound and stabilized WASF3, a protein implicated in actin polymerization, cell movement and metastasis. This group showed inhibition of Hsp72 to result in WASF3 protein destabilization and reduced invasive properties in breast cancer

cells. Chemical inhibition of Hsp72 activity led to loss of WASF3 in mammary tumor cells (Gong, J. et al, data not shown). Other proteins implicated in Hsp72-mediated cell migration and metastasis include tissue transglutaminase and MMP2 (50). Consistent with these reports, our studies implicated the *hsp70* gene in dissemination of mammary cancer cells to the lung (Figure 3). *hsp70* knockout also reduced mammary tumor cell migration (Figure 4). In addition, the CD44/Sca1^{+} cell population appeared to be important in mammary tumor cell migration and dissemination and these properties of CD44/Sca1^{+} cells far exceeded those in unsorted and CD44/Sca1^{-} cells (Figure 1c). Knockout of *hsp70* reduced the expression and activity of c-Met (Table 2 and Figure 6). The c-Met/Hgf signaling system was shown to play important roles in development (51, 52), as well as wound healing (53, 54). Skeletal muscles of the limb and diaphragm did not form because of the migratory impairment of myogenic precursor cells from dermo-myotome in the somites into the limb anlage and diaphragm in c-Met homozygous mutant (−/−) mouse embryos (51). Likewise, mice in which the gene encoding c-Met had been deleted from keratinocytes showed strongly delayed re-epithelialization in response to skin wounds (53). The c-Met/Hgf complex exerted key physiological functions in embryonic development and wound healing by promoting cell migration, survival and proliferation through an intricate system of signaling cascade (48). This strategy for development and organ regeneration could be hijacked in cancer and may be important for the properties of CSC. Indeed, c-Met/Hgf interactions were shown to play a central role in the invasive growth of tumors and in metastasis (52, 55–57). Autocrine activation of c-Met resulted in the development of malignant melanoma and mammary carcinoma with metastatic behavior in animal models of cancer (58, 59). Expression of c-Met in human cancers correlated with metastasis and poor prognosis (52, 57, 60–62). Together, our experiments suggest that the impaired tumorigenesis and lung metastasis in *hsp70*$^{-/-}$MMT mice might involve the combined results of a reduced pool of CSC and the downregulation of genes critical for invasive growth.

The mechanisms behind the pleiotropic effects of the *hsp70* gene on gene expression are not clear. However, Hsp72 has been shown to bind the transcriptional co-repressor Co-REST and may thus mediate gene repression directly (63). Hsp72 was also shown to function at the posttranscriptional level in stabilizing selected mRNAs and thus modulating gene expression by promotion of mRNA longevity (64). In addition, Hsp70 was shown recently to bind to Bag-3 and could in this way influence multiple pathways of signaling that might lead indirectly to effects on gene expression (23). Pleiotropy would thus be anticipated.

One notable message from the expression profiling studies in Table 2 was that the effects of Hsp72 would not be exclusively predicted to promote metastasis or tumorigenesis. For instance, matrix metalloproteinases Mmp11, Mmp3, Mmp9, known to be involved in tumor cell invasion and metastasis appeared to be repressed by *hsp70* (65). In addition the primary gene repressed by *hsp70* knockout was *timp4* that encodes *tissue inhibitor of matrix metalloproteinase 4* (Timp4), a protein that specifically inhibits Mmps. However in this case, Timp4 has, paradoxically, been shown to be abundantly expressed in metastatic breast tumors and may possess additional functions in addition to Mmp inhibition (66). In a recent paper by Colvin et al (23), it was shown that Hsp72 appeared to function in carcinogenesis by interacting with Bag-3 and that, while the aggregate effects of Hsp72 promoted

tumorigenesis, some of the molecular effects that were observed might be expected to reduce cancer formation. The combined weight of the gene expression changes induced by Hsp72 appeared however to favor tumorigenesis and metastasis. Our data suggested a similar conclusion, that while Hsp72 expression overall promoted the CSC and metastatic properties of MMT cells, some contrary effects on gene expression were observed (Table 2).

The findings reported here, showing Hsp72 to mediate a stem cell and metastatic phenotype in mammary cancer might have potential clinical significance since metastasis was shown to be a major cause of mortality in breast cancer patients. The current studies thus suggested Hsp72, as well as c-Met, to be a potential target for new tumor therapies. Hsp72 could be attractive for cancer drug development since the *hsp70*$^{-/-}$MMT showed a remarkably reduced rate of spontaneous metastasis and were viable and healthy, indicating minimal toxicity.

Materials and Methods

Mice and in vivo study

Animal maintenance and experiments were conducted in compliance with IACUC guidelines. Animals were maintained in microisolator cages under specific pathogen-free conditions. The mice (C57BL/6 background) used in our experiments included female mice double transgenic for the polyomavirus middle T (PyMT) oncogene driven by the mouse mammary tumor virus long terminal repeat (MMTV-LTR) and the human MUC1 antigen (mucin 1) (a kind gift from Sandra J. Gendler, Mayo Clinic, Scottsdale, AZ, USA). Mice expressing PyMT developed mammary carcinomas, and the MUC1 antigen was expressed in a tissue-specific fashion similar to that in humans. Hsp70 knockout mice (*hsp70*$^{-/-}$ mice in C57/129 background) were obtained from Dr. Clayton Hunt (Washington University, St Louis, MO, USA) and back crossed over the C57BL/6 strain. *hsp70*$^{-/-}$ mice were mated with MMT mice to generate *hsp70*$^{+/-}$MMT and *hsp70*$^{-/-}$MMT mice. Wild-type (WT) female C57BL/6 mice (C57BL/6NTac) were purchased from Taconic Farms (Germantown, NY, USA) and used as recipient mice to determine tumorigenic and metastatic potential.

The *in vivo* studies were performed as previously described (34). Briefly, mammary tumor cells isolated from MMT, *hsp70*$^{+/-}$MMT and *hsp70*$^{-/-}$MMT mice were cultured in Dulbecco's Modification of Eagle's Medium™ (DMEM) with 4.5g/L glucose and 2mM L-glutamine supplemented with 10% fetal calf serum (FCS), and 100μg/ml of both penicillin and streptomycin (Cellgro, Mediatech, Inc., Manassas, VA) overnight, and then harvested and injected into the fat pads of mammary glands of WT mice (10^6 tumor cells). The mice were followed for up to 30 days to monitor tumor growth.

PCR for gene detection and phenotyping

PCR analysis was used to confirm the presence of the MUC1, *PyMT* and *hsp70* genes in transgenic mice. Tail tissue DNA was extracted using the REDExtrac-N-Amp Tissue PCR Kit(Sigma, Steinheim, Germany). 100nM 5'-AGTCACTGCTACTGCACCCAG-3' forward primer and 5'-CTCTCCTCAGTTCCTCGCTCC-3' reverse primers were used for the MT gene and 5'-CTTGCCAGCCATAGCACCAAG-3' and 5'-

CTCCACGTCGTGGACATTGATG-3' for the MUC1 gene. Primers for the detection of the *hsp70* gene included 5'- AGCTGTGCTCGGACCTGTT −3' (forward), 5'-GCTTGCCCTTGAGACCCT −3' (reverse), and internal positive control 5'-ACTGAAGCGGGAAGGGACT −3' (forward), 5'- CGGCGATACCGTAAAGCAC −3' (reverse). PCR was carried out using these primers as well as the additional reagents: 10μl 2 × PCR mix, 4μl tail DNA, and reagent quality H_20. Size fractionation in a 1% agarose gel was used to analyze the PCR products.

Immunocytochemical or immunohistochemical staining

Cells from spontaneous mammary tumors were isolated from MMT mice and incubated overnight in DMEM with 4.5g/L glucose and 2mM L-glutamine supplemented with 10% FCS, and 100μg/ml of both penicillin and streptomycin (Cellgro, Mediatech) in a Heracell CO_2 incubator at 37°C and 5% CO_2. The tumor cells were collected and stained with antibodies against CD44 (clone IM7) and Sca1 (clone D7) (e-Bioscience, Inc., San Diego, CA), and then sorted into CD44/Sca1$^+$ and CD44/Sca1$^-$ subsets. The sorted cells were further stained with antibodies against HSF1 regulated protein (clone 10H8, Enzo Life Sciences), HSF1 phosphorylated on serine 326 (phospho-HSF1-S326, clone EP1713Y, Abcam, Cambridge, MA), HSP70 (Ab46) (67), metastasis associated protein 1 (MTA1, Abcam), and/or epithelial specific antigen (ESA, clone G8.8) (e-Bioscience) using standard immunocytochemical (ICC) staining method. Ab46 was produced by the Calderwood lab targeting an epitope encompassing the C-terminal 16 amino acids of Hsp72. This antibody recognizes both mouse and human Hsp72 with high affinity and is functional in immunoblot, immunoprecipitation and immmunohistochemistry.

To determine the activity of c-Met in mammary tumors, frozen sections of tumors from MMT and *hsp70*$^{-/-}$MMT mice were stained with mAbs against phosphorylated c-Met (Y1349, R&D Systems, Minneapolis, MN), CD44 (clone IM7) and/or Sca1 (clone D7) (e-Bioscience) in either single or double staining using standard immunohistochemical staining methods. Briefly, frozen sections were air-dried, fixed in acetone and incubated with anti-p-Met antibody at 1:100 dilutions for 1 hr at room temperature. After the slides were washed, biotinylated goat anti-rabbit IgG was applied for an additional 45 min. The positive cells were stained red with ABC solution (Vector Laboratories, Burlingame, CA). The slides were further incubated with anti-Sca1 or CD44 mAbs for 1 hr at room temperature. After 1x PBS wash, the slides were incubated with biotinylated rabbit anti-rat IgG for 45 min, and then followed by alkaline phosphatase (AP-ABC) solution (Vector Laboratories) to generate a blue color. The slides were examined under a microscope.

Western Blotting

Lysates obtained from mammary tumor cells were subjected to SDS-PAGE followed by standard western blot procedure. The following antibodies were used for analysis of protein expression: anti-HSP70, HSP90 (SPA-830), HSP110 (SPA-1103) (Stressgen, Ann Arbor, MI), HSF1, HSF1 phospho-Serine 326 (Abcam) and β-actin (Sigma). Secondary antibodies used were horseradish peroxidase-goat anti-mouse IgG, horseradish peroxidase goat anti-rabbit IgG (Santa Cruz, Dallas, Texas). The Ag/Ab complexes were visualized by ECL

(ECL Detection System; GE). Densitometric analysis of the membranes was performed using GelDoc 2000 (Bio-Rad, Hercules, CA).

Histological examination with whole mount and ESA staining

Mice were sacrificed at the indicated ages. For whole mount preparation, thoracic mammary glands were harvested and resected tissue was spread onto a slide and fixed in Carnoy's fixative (60% ethanol, 30% chloroform, 10% glacial acetic acid) for 2 to 4 hours at 4°C. The tissue mount was washed in 70% ethanol for 15 min, 50% ethanol for 15 min, rinsed with distilled water for 5 min and placed in a Carmine Alum staining solution over night. Stained whole mammary glands were kept in 70% ethanol at 4°C for photograph. The hyperplastic epithelial nodules or tumor masses (greater than 1 mm^2 areas) as indicated by the deep red-staining with Carmine Alum were measured using Spot Advanced™ digital imaging software (Diagnostic Instruments, Inc., Sterling Heights, MI, USA). Mammary glands were then paraffin-embedded, sectioned (5 μm), stained with anti-ESA mAb (clone G8.8) (e-Bioscience) and examined under a light microscope.

To visualize lung metastases, the lungs harvested from MMT mice with or without Hsp72, sectioned (5 μm) and stained with hematoxylin and eosin (H&E). The slides were examined under a light microscope.

Clonogenic assay for lung dissemination

To identify the presence of disseminated cells in the lungs, the clonogenic assay was used as described previously (34). Briefly, a 24G needle was used to perfuse the lungs of blood with sterile PBS via the right ventricle of the heart before harvesting the lung tissue. The lungs were collected, minced and digested in a collagenase enzyme cocktail solution. Single cells were cultured in DMEM with 10% FCS for two weeks. Presence of disseminated or metastatic tumor cells was determined by growth of tumor colonies on tissue culture plates and colonies were detected with 0.5% crystal violet staining. Each colony (>50 cells) was counted to quantify the number of disseminated cells for each individual mouse.

Cell viability assay

Mammary tumor cells were isolated from MMT, *hsp70*$^{+/-}$MMT and *hsp70*$^{-/-}$MMT mice (age > 95 days) as previously described (43). Briefly, tumors harvested from mice were minced into small pieces (1–3 mm) and digested in Hank's Balanced Salt Solution (HBSS, Cellgro, Mediatech) containing collagenase and DNase. The digested tumor tissue was mashed through a sterile 50-μm nylon mesher using sterile technique, in a tissue culture hood. Single-tumor cell suspensions were obtained by passing through a filter. The tumor cells were then cultured at 37°C in DMEM with 4.5g/L glucose and 2mM L-glutamine supplemented with 10% heat-inactivated FCS, 100μg/ml of both penicillin and streptomycin. After overnight culture, the nonadherent and dead cells were removed, and fresh medium was added. Seventy-two hours after incubation, a 20-μl aliquot of MTT solution (5 mg/ml in PBS) was added to each well and incubated for another 4 h, followed by centrifugation at 800 rpm for 5 min. The supernatant in the culture was carefully aspirated, and 200 μl DMSO was added to each well and shaken for 10 min to dissolve the formazan crystals. The absorbance was measured at 590 nm by a microplate reader (68). Cell viability was

calculated as the percentage of MTT absorption as follows: percentage survival = (mean experimental absorbance/mean control absorbance) × 100%.

Cell migration assays

Wound healing and multiwell cell migration assays were used to measure migratory ability. The would healing assay was performed as described with minor modification (69). The multiwell cell migration assay involves two chambers that are separated by a porous filter (40). Cells were placed in the upper chamber and incubated. Cells that migrated through the pores of the filter toward to the underside of the filter were considered to possess migratory capacity. The sorted CD44/Sca1^{+}, CD44/Sca1^{-} cells and unsorted tumor cells were placed onto a filter on a cell chamber and cultured. At the indicated times, the filters were gently removed. The cells in the upper side of filter were removed and those under side were then fixed and stained with 0.5% crystal violet. The filter was photographed at 10x and the cells were counted

Metastasis-related gene expression profiling

Tumor tissues were obtained from MMT and *hsp70*$^{-/-}$MMT mice. Tissues were ground and lysed in Quazol (Qiagen, Valencia, CA). Total RNA was prepared using miRNeasy mini columns (Qiagen) and RNA concentration then measured by NanoDrop (Thermo). For both gene expression profiling and qRT-PCR, 5μg of total RNA was used. Procedures involved genomic DNA elimination followed by reverse transcription carried out using an RT2 first strand kit (Qiagen). An RT2 profiler PCR array for mouse tumor metastasis (Qiagen) was used for gene expression profiling. 89 genes including 5 housekeeping genes were analyzed for 2 tumor regions each in MMT and *hsp70*$^{-/-}$MMT mice. Threshold for analysis of Ct value were adjusted between samples based on Ct in house keeping genes. The means of 2 values were compared. The qRT-PCR was performed and the primers designed as previously described (70). The cDNA synthesized was diluted by adding 91μl of water before realtime PCR. The diluted cDNA was further 10-fold diluted for realtime PCR for control 18s rRNA. cDNA (3μl) and primers (0.25μM each) were used in 20μl of realtime PCR reaction. The primer pairs for *mhsp70.1/a1b* (F): gctcgagtcctatgccttca; *mhsp70.1/a1b* (R): atgacctcctggcacttgtc; *mhsp70.3/a1a* (F): gatttgttttgcaggacagc; *mhsp70.3/a1a* (R): ggggagagtccaaacacaaa; *mMet* (F): aagaaaatgaatgcgccaat; *mMe*t (R): tgtccagacacattgcccta; *mHgf* (F): tgttccatgtgggacaagaa; *mHgf* (R): aagaggattccccgtgtagc

Statistical Analysis

Statistical significance was determined using Student's *t*-test or X^2-test. One way analysis of variance (ANOVA) was used for analysis of data with more than two subgroups. *P*-values of <0.05 were considered statistically significant. The statistical analysis software, SPSS Statistics™ v17.0 (IBM Corporation, Somer, NY), was used to attain these values.

Supplementary Material

Refer to Web version on PubMed Central for supplementary material.

Acknowledgment

We acknowledge the support of the Department of Radiation Oncology, Beth Israel Deaconess Medical Center. This work was supported by NIH research grants R01CA119045, RO1CA47407 and RO1CA176326 as well as the Harvard JCRT Foundation. We are grateful to Buzz Hunt for the kind gift of the *hsp70* knockout mice.

Source of support

This work was supported by the funding from NIH research grants R01CA119045, RO1CA47407 and RO1CA176326.

References

1. Hanahan D, Weinberg RA. Hallmarks of cancer: the next generation. Cell. 2011;144(5):646–74. [PubMed: 21376230]
2. Dang CV. Links between metabolism and cancer. Genes & development. 2012;26(9):877–90. [PubMed: 22549953]
3. Calderwood SK. Molecular Cochaperones: Tumor Growth and Cancer Treatment. Scientifica. 2013;2013:217513. [PubMed: 24278769]
4. Calderwood SK, Gong J. Molecular chaperones in mammary cancer growth and breast tumor therapy. Journal of cellular biochemistry. 2012;113(4):1096–103. [PubMed: 22105880]
5. Craig EA. The heat shock response. CRC critical reviews in biochemistry. 1985;18(3):239–80. [PubMed: 2412760]
6. Ciocca DR, Calderwood SK. Heat shock proteins in cancer: diagnostic, prognostic, predictive, and treatment implications. Cell Stress Chaperones. 2005;10(2):86–103. [PubMed: 16038406]
7. Modi S, Stopeck AT, Gordon MS, Mendelson D, Solit DB, Bagatell R, et al. Combination of trastuzumab and tanespimycin (17-AAG, KOS-953) is safe and active in trastuzumab-refractory HER-2 overexpressing breast cancer: a phase I dose-escalation study. J Clin Oncol. 2007;25(34):5410–7. [PubMed: 18048823]
8. Modi S, Stopeck A, Linden H, Solit D, Chandarlapaty S, Rosen N, et al. HSP90 inhibition is effective in breast cancer: a phase II trial of tanespimycin (17-AAG) plus trastuzumab in patients with HER2-positive metastatic breast cancer progressing on trastuzumab. Clin Cancer Res. 2011;17(15):5132–9. [PubMed: 21558407]
9. Neckers L, Workman P. Hsp90 molecular chaperone inhibitors: are we there yet? Clinical cancer research : an official journal of the American Association for Cancer Research. 2012;18(1):64–76. [PubMed: 22215907]
10. Barrott JJ, Haystead TA. Hsp90, an unlikely ally in the war on cancer. The FEBS journal. 2013;280(6):1381–96. [PubMed: 23356585]
11. Powers MV, Jones K, Barillari C, Westwood I, van Montfort RL, Workman P. Targeting HSP70: the second potentially druggable heat shock protein and molecular chaperone? Cell cycle. 2010;9(8):1542–50. [PubMed: 20372081]
12. Goloudina AR, Demidov ON, Garrido C. Inhibition of HSP70: a challenging anti-cancer strategy. Cancer Lett. 2012;325(2):117–24. [PubMed: 22750096]
13. Galluzzi L, Giordanetto F, Kroemer G. Targeting HSP70 for cancer therapy. Mol Cell. 2009;36(2):176–7. [PubMed: 19854128]
14. Lindquist S, Craig EA. The heat-shock proteins. Annu Rev Genet. 1988;22:631–77. [PubMed: 2853609]
15. Bukau B, Horwich AL. The Hsp70 and Hsp60 chaperone machines. Cell. 1998;92(3):351–66. [PubMed: 9476895]
16. Tang D, Khaleque MA, Jones EL, Theriault JR, Li C, Wong WH, et al. Expression of heat shock proteins and heat shock protein messenger ribonucleic acid in human prostate carcinoma in vitro and in tumors in vivo. Cell stress & chaperones. 2005;10(1):46–58. [PubMed: 15832947]
17. Schlesinger MJ. How the cell copes with stress and the function of heat shock proteins. Pediatr Res. 1994;36(1 Pt 1):1–6. [PubMed: 7936827]

18. Hunt CR, Dix DJ, Sharma GG, Pandita RK, Gupta A, Funk M, et al. Genomic instability and enhanced radiosensitivity in Hsp70.1- and Hsp70.3-deficient mice. Molecular and cellular biology. 2004;24(2):899–911. [PubMed: 14701760]
19. Georgopoulos C, Welch WJ. Role of the major heat shock proteins as molecular chaperones. Annu Rev Cell Biol. 1993;9:601–34. [PubMed: 8280473]
20. Calderwood SK. HSF1, a versatile factor in tumorogenesis. Curr Mol Med. 2012;12(9):1102–7. [PubMed: 22804234]
21. Rerole AL, Jego G, Garrido C. Hsp70: anti-apoptotic and tumorigenic protein. Methods Mol Biol. 2011;787:205–30. [PubMed: 21898238]
22. Gao T, Newton AC. The turn motif is a phosphorylation switch that regulates the binding of Hsp70 to protein kinase C. J Biol Chem. 2002;277(35):31585–92. [PubMed: 12080070]
23. Colvin TA, Gabai VL, Gong J, Calderwood SK, Li H, Gummuluru S, et al. Hsp70-bag3 interactions regulate cancer-related signaling networks. Cancer Res. 2014;74(17):4731–40. [PubMed: 24994713]
24. Kang Y, Jung WY, Lee H, Jung W, Lee E, Shin BK, et al. Prognostic significance of heat shock protein 70 expression in early gastric carcinoma. Korean J Pathol. 2013;47(3):219–26. [PubMed: 23837014]
25. Kluger HM, Chelouche Lev D, Kluger Y, McCarthy MM, Kiriakova G, Camp RL, et al. Using a xenograft model of human breast cancer metastasis to find genes associated with clinically aggressive disease. Cancer Res. 2005;65(13):5578–87. [PubMed: 15994930]
26. Sun B, Zhang S, Zhang D, Li Y, Zhao X, Luo Y, et al. Identification of metastasis-related proteins and their clinical relevance to triple-negative human breast cancer. Clin Cancer Res. 2008;14(21):7050–9. [PubMed: 18981002]
27. Kalogeraki A, Giannikaki E, Tzardi M, Kafousi M, Ieromonachou P, Dariviannaki K, et al. Correlation of heat shock protein (HSP70) expression with cell proliferation (MIB1), estrogen receptors (ER) and clinicopathological variables in invasive ductal breast carcinomas. J Exp Clin Cancer Res. 2007;26(3):367–8. [PubMed: 17987797]
28. Rohde M, Daugaard M, Jensen MH, Helin K, Nylandsted J, Jaattela M. Members of the heat-shock protein 70 family promote cancer cell growth by distinct mechanisms. Genes Dev. 2005;19(5):570–82. [PubMed: 15741319]
29. Thanner F, Sutterlin MW, Kapp M, Rieger L, Kristen P, Dietl J, et al. Heat-shock protein 70 as a prognostic marker in node-negative breast cancer. Anticancer Res. 2003;23(2A):1057–62. [PubMed: 12820347]
30. Nakajima M, Kuwano H, Miyazaki T, Masuda N, Kato H. Significant correlation between expression of heat shock proteins 27, 70 and lymphocyte infiltration in esophageal squamous cell carcinoma. Cancer Lett. 2002;178(1):99–106. [PubMed: 11849747]
31. Liu FF, Miller N, Levin W, Zanke B, Cooper B, Henry M, et al. The potential role of HSP70 as an indicator of response to radiation and hyperthermia treatments for recurrent breast cancer. Int J Hyperthermia. 1996;12(2):197–208. [PubMed: 8926389]
32. Pocaly M, Lagarde V, Etienne G, Ribeil JA, Claverol S, Bonneu M, et al. Overexpression of the heat-shock protein 70 is associated to imatinib resistance in chronic myeloid leukemia. Leukemia. 2007;21(1):93–101. [PubMed: 17109025]
33. Guy CT, Cardiff RD, Muller WJ. Induction of mammary tumors by expression of polyomavirus middle T oncogene: a transgenic mouse model for metastatic disease. Mol Cell Biol. 1992;12(3):954–61. [PubMed: 1312220]
34. Weng D, Penzner JH, Song B, Koido S, Calderwood SK, Gong J. Metastasis is an early event in mouse mammary carcinomas and is associated with cells bearing stem cell markers. Breast Cancer Res. 2012;14(1):R18. [PubMed: 22277639]
35. Grange C, Lanzardo S, Cavallo F, Camussi G, Bussolati B. Sca-1 identifies the tumor-initiating cells in mammary tumors of BALB-neuT transgenic mice. Neoplasia. 2008;10(12):1433–43. [PubMed: 19048122]
36. Li F, Tiede B, Massague J, Kang Y. Beyond tumorigenesis: cancer stem cells in metastasis. Cell Res. 2007;17(1):3–14. [PubMed: 17179981]

37. Santagata S, Hu R, Lin NU, Mendillo ML, Collins LC, Hankinson SE, et al. High levels of nuclear heat-shock factor 1 (HSF1) are associated with poor prognosis in breast cancer. Proceedings of the National Academy of Sciences of the United States of America. 2011;108(45):18378–83. [PubMed: 22042860]
38. Chou SD, Prince T, Gong J, Calderwood SK. mTOR is essential for the proteotoxic stress response, HSF1 activation and heat shock protein synthesis. PLoS One. 2012;7(6):e39679. [PubMed: 22768106]
39. Khaleque MA, Bharti A, Gong J, Gray PJ, Sachdev V, Ciocca DR, et al. Heat shock factor 1 represses estrogen-dependent transcription through association with MTA1. Oncogene. 2008;27(13):1886–93. [PubMed: 17922035]
40. Kouspou MM, Price JT. Analysis of cellular migration using a two-chamber methodology. Methods Mol Biol. 2011;787:303–17. [PubMed: 21898245]
41. Guy CT, Muthuswamy SK, Cardiff RD, Soriano P, Muller WJ. Activation of the c-Src tyrosine kinase is required for the induction of mammary tumors in transgenic mice. Genes Dev. 1994;8(1):23–32. [PubMed: 7507074]
42. Mukherjee P, Madsen CS, Ginardi AR, Tinder TL, Jacobs F, Parker J, et al. Mucin 1-specific immunotherapy in a mouse model of spontaneous breast cancer. J Immunother. 2003;26(1):47–62. [PubMed: 12514429]
43. Xia J, Tanaka Y, Koido S, Liu C, Mukherjee P, Gendler SJ, et al. Prevention of spontaneous breast carcinoma by prophylactic vaccination with dendritic/tumor fusion cells. J Immunol. 2003;170(4):1980–6. [PubMed: 12574367]
44. Lengyel E, Prechtel D, Resau JH, Gauger K, Welk A, Lindemann K, et al. C-Met overexpression in node-positive breast cancer identifies patients with poor clinical outcome independent of Her2/neu. International journal of cancer Journal international du cancer. 2005;113(4):678–82. [PubMed: 15455388]
45. Locatelli A, Lofgren KA, Daniel AR, Castro NE, Lange CA. Mechanisms of HGF/Met signaling to Brk and Sam68 in breast cancer progression. Hormones & cancer. 2012;3(1–2):14–25. [PubMed: 22124844]
46. Meng L, Hunt C, Yaglom JA, Gabai VL, Sherman MY. Heat shock protein Hsp72 plays an essential role in Her2-induced mammary tumorigenesis. Oncogene. 2011;30(25):2836–45. [PubMed: 21297664]
47. Cardiff RD, Muller WJ. Transgenic mouse models of mammary tumorigenesis. Cancer Surv. 1993;16:97–113. [PubMed: 8394206]
48. Trusolino L, Bertotti A, Comoglio PM. MET signalling: principles and functions in development, organ regeneration and cancer. Nat Rev Mol Cell Biol. 2010;11(12):834–48. [PubMed: 21102609]
49. Teng Y, Ngoka L, Mei Y, Lesoon L, Cowell JK. HSP90 and HSP70 proteins are essential for stabilization and activation of WASF3 metastasis-promoting protein. J Biol Chem. 2012;287(13):10051–9. [PubMed: 22315230]
50. Boroughs LK, Antonyak MA, Johnson JL, Cerione RA. A unique role for heat shock protein 70 and its binding partner tissue transglutaminase in cancer cell migration. J Biol Chem. 2011;286(43):37094–107. [PubMed: 21896482]
51. Bladt F, Riethmacher D, Isenmann S, Aguzzi A, Birchmeier C. Essential role for the c-met receptor in the migration of myogenic precursor cells into the limb bud. Nature. 1995;376(6543):768–71. [PubMed: 7651534]
52. Birchmeier C, Birchmeier W, Gherardi E, Vande Woude GF. Met, metastasis, motility and more. Nat Rev Mol Cell Biol. 2003;4(12):915–25. [PubMed: 14685170]
53. Chmielowiec J, Borowiak M, Morkel M, Stradal T, Munz B, Werner S, et al. c-Met is essential for wound healing in the skin. J Cell Biol. 2007;177(1):151–62. [PubMed: 17403932]
54. Gurtner GC, Werner S, Barrandon Y, Longaker MT. Wound repair and regeneration. Nature. 2008;453(7193):314–21. [PubMed: 18480812]
55. Weidner KM, Behrens J, Vandekerckhove J, Birchmeier W. Scatter factor: molecular characteristics and effect on the invasiveness of epithelial cells. J Cell Biol. 1990;111(5 Pt 1):2097–108. [PubMed: 2146276]

56. Thiery JP. Epithelial-mesenchymal transitions in tumour progression. Nat Rev Cancer. 2002;2(6):442–54. [PubMed: 12189386]
57. Boccaccio C, Comoglio PM. Invasive growth: a MET-driven genetic programme for cancer and stem cells. Nat Rev Cancer. 2006;6(8):637–45. [PubMed: 16862193]
58. Gallego MI, Bierie B, Hennighausen L. Targeted expression of HGF/SF in mouse mammary epithelium leads to metastatic adenosquamous carcinomas through the activation of multiple signal transduction pathways. Oncogene. 2003;22(52):8498–508. [PubMed: 14627990]
59. Otsuka T, Takayama H, Sharp R, Celli G, LaRochelle WJ, Bottaro DP, et al. c-Met autocrine activation induces development of malignant melanoma and acquisition of the metastatic phenotype. Cancer Res. 1998;58(22):5157–67. [PubMed: 9823327]
60. Ghoussoub RA, Dillon DA, D'Aquila T, Rimm EB, Fearon ER, Rimm DL. Expression of c-met is a strong independent prognostic factor in breast carcinoma. Cancer. 1998;82(8):1513–20. [PubMed: 9554529]
61. Lee WY, Chen HH, Chow NH, Su WC, Lin PW, Guo HR. Prognostic significance of co-expression of RON and MET receptors in node-negative breast cancer patients. Clin Cancer Res. 2005;11(6):2222–8. [PubMed: 15788670]
62. Takeuchi H, Bilchik A, Saha S, Turner R, Wiese D, Tanaka M, et al. c-MET expression level in primary colon cancer: a predictor of tumor invasion and lymph node metastases. Clin Cancer Res. 2003;9(4):1480–8. [PubMed: 12684423]
63. Gomez AV, Galleguillos D, Maass JC, Battaglioli E, Kukuljan M, Andres ME. CoREST represses the heat shock response mediated by HSF1. Molecular cell. 2008;31(2):222–31. [PubMed: 18657505]
64. Kishor A, Tandukar B, Ly YV, Toth EA, Suarez Y, Brewer G, et al. Hsp70 is a novel posttranscriptional regulator of gene expression that binds and stabilizes selected mRNAs containing AU-rich elements. Molecular and cellular biology. 2013;33(1):71–84. [PubMed: 23109422]
65. Slattery ML, John E, Torres-Mejia G, Stern M, Lundgreen A, Hines L, et al. Matrix metalloproteinase genes are associated with breast cancer risk and survival: the Breast Cancer Health Disparities Study. PloS one. 2013;8(5):e63165. [PubMed: 23696797]
66. Jiang Y, Wang M, Celiker MY, Liu YE, Sang QX, Goldberg ID, et al. Stimulation of mammary tumorigenesis by systemic tissue inhibitor of matrix metalloproteinase 4 gene delivery. Cancer research. 2001;61(6):2365–70. [PubMed: 11289097]
67. Stevenson MA, Calderwood SK. Members of the 70-kilodalton heat shock protein family contain a highly conserved calmodulin-binding domain. Mol Cell Biol. 1990;10(3):1234–8. [PubMed: 2154682]
68. Weng D, Song B, Koido S, Calderwood SK, Gong J. Immunotherapy of radioresistant mammary tumors with early metastasis using molecular chaperone vaccines combined with ionizing radiation. J Immunol. 2013;191(2):755–63. [PubMed: 23772032]
69. Rodriguez LG, Wu X, Guan JL. Wound-healing assay. Methods Mol Biol. 2005;294:23–9. [PubMed: 15576902]
70. Eguchi T, Watanabe K, Hara ES, Ono M, Kuboki T, Calderwood SK. OstemiR: a novel panel of microRNA biomarkers in osteoblastic and osteocytic differentiation from mesencymal stem cells. PLoS One. 2013;8(3):e58796. [PubMed: 23533592]

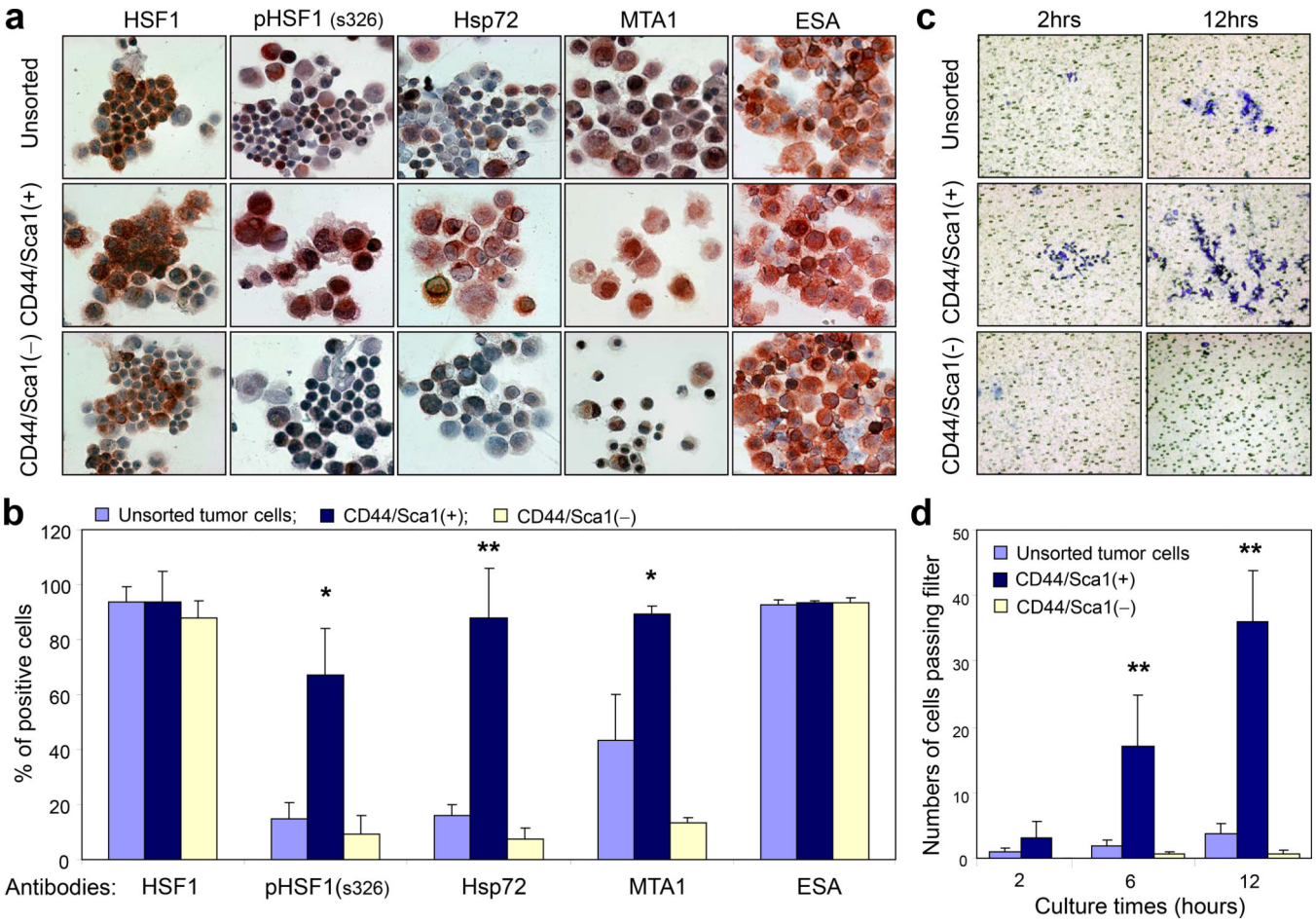

Figure 1. Hsp72 and HSF1 network expression in CD44/Sca1$^+$ cells from mammary tumors.

Mammary tumor cells were isolated from MMT mice at ages of 112–132 days. The tumor cells were stained with anti-CD44 and anti-Sca1 mAbs and selected by cell sorting. (**a**) The sorted CD44/Sca1$^+$, CD44/Sca1$^-$ cells and unsorted tumor cells were further stained with anti-HSF1, pHSF1, Hsp72, MTA1 and ESA mAbs using immunohistochemical staining. Positive cells were stained red (60x). (**b**) The positive cells were counted and shown in 3 bars (unsorted cells, CD44/Sca1 (+) and CD44/Sca1 (−)) from repeated experiments. Percentage of positive cells was presented in bar graph and the error bar represents standard deviation. (**c**) The sorted CD44/Sca1$^+$, CD44/Sca1$^-$ cells and unsorted tumor cells were placed on the filter of upper side of a migration chamber and cultured. At the indicated times, the filters were gently removed and the cells on the upper side of filter were cleared. The cells in the lower side of filter were fixed with 4% paraformaldehyde and stained with 0.5% crystal violet. Filters were then photographed and the cells were counted under microscopy (10x). (**d**) The numbers of cells passing through the filter were presented in a bar graph from repeated experiments and error bar represented standard deviation. " * " and " ** " indicate $p<0.05$ *and* 0.01, respectively.

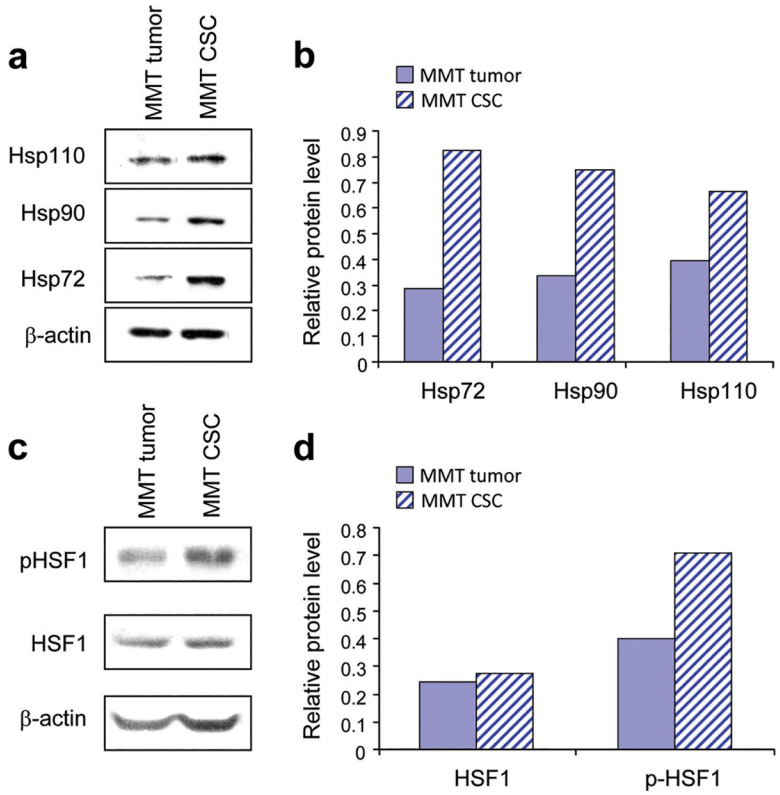

Figure 2. Measurement of HSP and HSF1 expression in CSC fractions.

Lysates were obtained from mammary tumor cells of MMT mice (MMT tumor) or the enriched CSC fraction. The lysates were analyzed by SDS-PAGE with equal loading and the expression levels of Hsp72, Hsp90 and Hsp110 (**a and b**), and HSF1 and pHSF1-S326 (**c and d**) were determined by western blotting. Expression levels of β-actin were also measured as loading controls. (**b and d**) were the merged quantitation of the protein levels from two experiments.

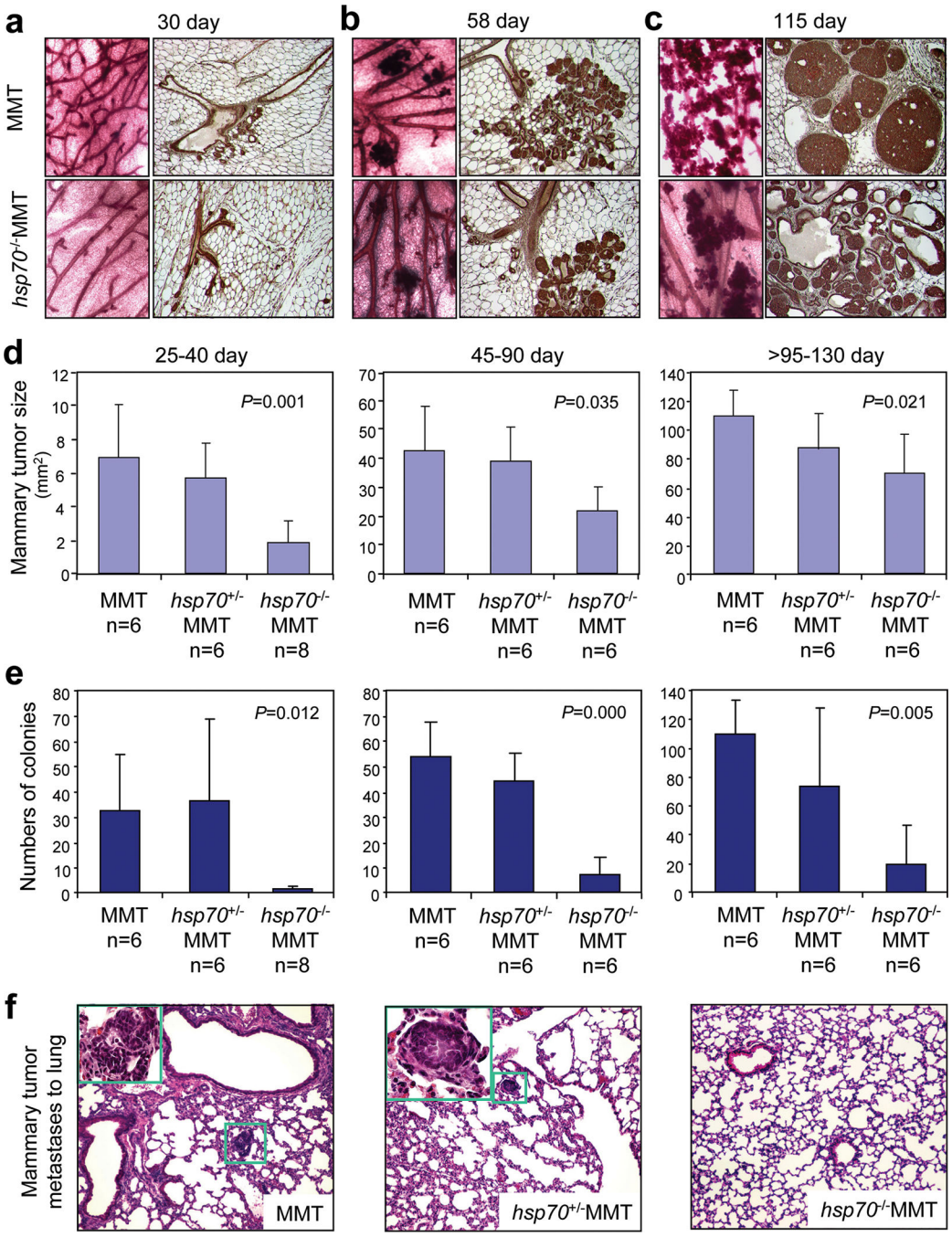

Figure 3, Development of primary mammary tumors and detection of metastatic cells in MMT mice with and without *hsp70* expression.

(**a-c**) Mammary glands were harvested from MMT, *hsp70*$^{+/-}$MMT and *hsp70*$^{-/-}$MMT mice at the indicated ages, processed for whole mount or sections that were stained with anti-ESA antibody. (**d**) Mammary epithelial nodules or masses in three different age groups (n= 6/ group) were compared using Spot Advanced™digital imaging software. The hyperplastic epithelial nodules were detected with Carmine Alum staining and greater than 1 mm^2 areas were measured and summarized. (**e**) Detection of disseminated cells in the mouse lungs.

Lungs were harvested from MMT, *hsp70*$^{+/-}$MMT and *hsp70*$^{-/-}$MMT mice, and perfused to remove the circulating cells. The lung tissue was minced and digested in a collagenase enzyme cocktail solution. The cells were then cultured for two weeks and stained with 0.5% crystal violet. Tumor colonies from lung cultures of each mouse (n= 6/group) were counted. >50 cells were considered as tumor cell colony. The error bars indicated standard deviation. Statistical analysis of the numbers of lung colonies from MMT, *hsp70*$^{+/-}$MMT and *hsp70*$^{-/-}$MMT mice in three age groups was performed using *one-way ANOVA*. (**f)** Lungs from MMT (110 day), *hsp70*$^{+/-}$MMT (110 day) and *hsp70*$^{-/-}$MMT (112 day) mice were processed for histological examination with H&E staining (10x). The green square indicated the enlarged area (60x).

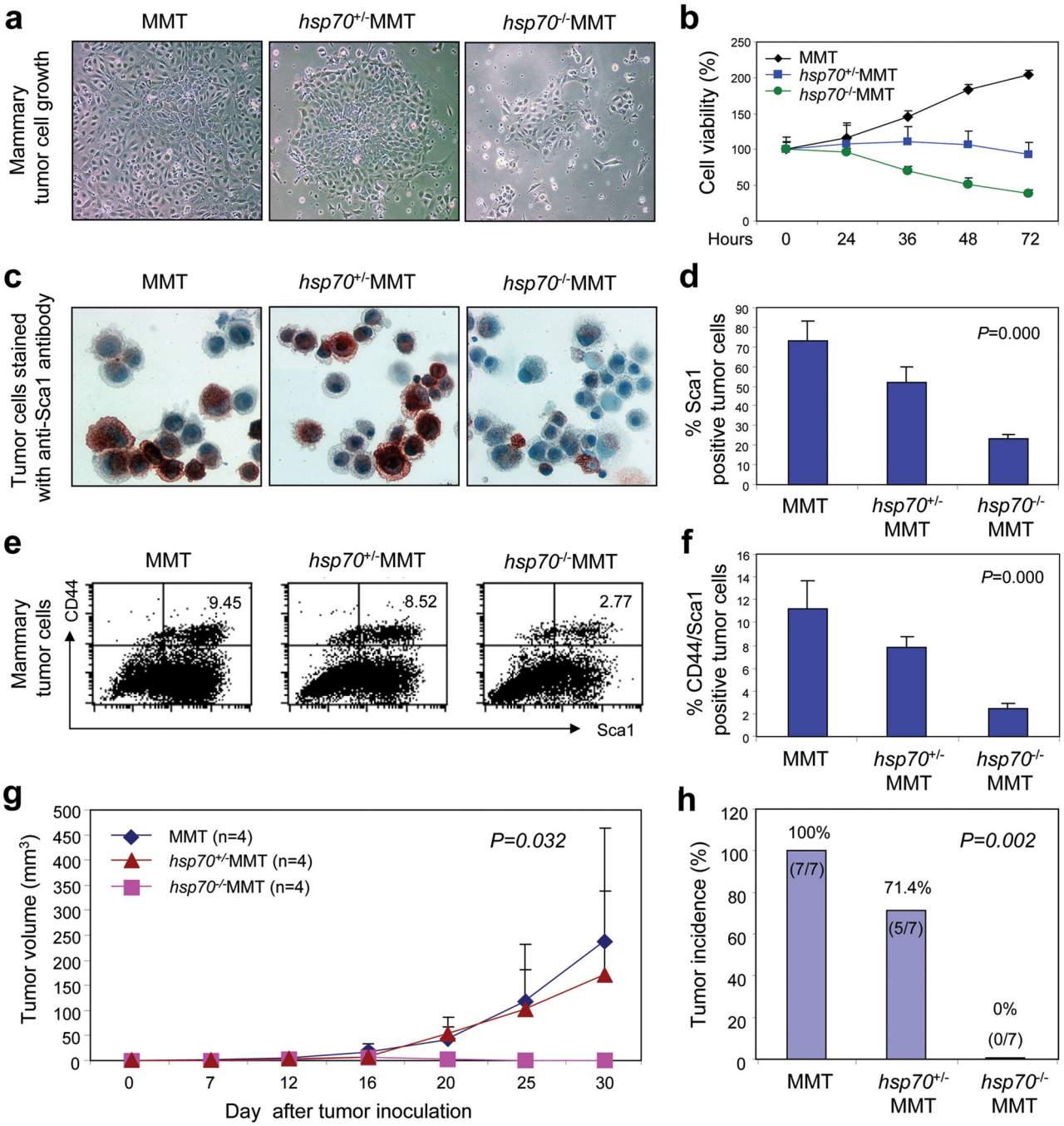

Figure 4. Reduced proliferation and numbers of Sca1+/CD44+ cells in mammary tumor cells from *hsp70* knockout mice.

Mammary tumor cells were isolated from MMT, *hsp70*$^{+/-}$MMT and *hsp70*$^{-/-}$MMT mice for phenotype and growth of CSC. (**a**) Mammary tumor cells were isolated, placed in the tissue culture plates (2×10^6 cells/plate), and cultured in DMEM for 36 hours and photographed under microscope. (**b**) Mammary tumor cells were placed in 96 well plates and cultured for 3 days. Cell viability was measured by MTT assay at the indicated times. (**c and d**) The cells were further stained with anti-Sca1 mAb using ICC staining **(c).** The positive cells were

counted and presented in a bar graph **(d).** (**e and f**) The mammary tumor cells were stained with anti-CD44 and -Sca1 mAbs and analyzed by FACS. The percentage of CD44/Sca1 positive cells was presented in the bar graph. (**b**, **d** and **f)** The results were summary of three experiments. The error bars indicated standard deviation. *P* values were obtained by X^2-test. (**g and h**) 1×10^6 tumor cells from MMT, *hsp70*$^{+/-}$MMT and *hsp70*$^{-/-}$MMT mice were injected into the fat pads of mammary glands of WT mice. The tumor growth was checked and tumor incidence was determined on day 30 after tumor inoculation. The tumor incidence was presented in bar graph. Statistical analysis was performed using X^2-test.

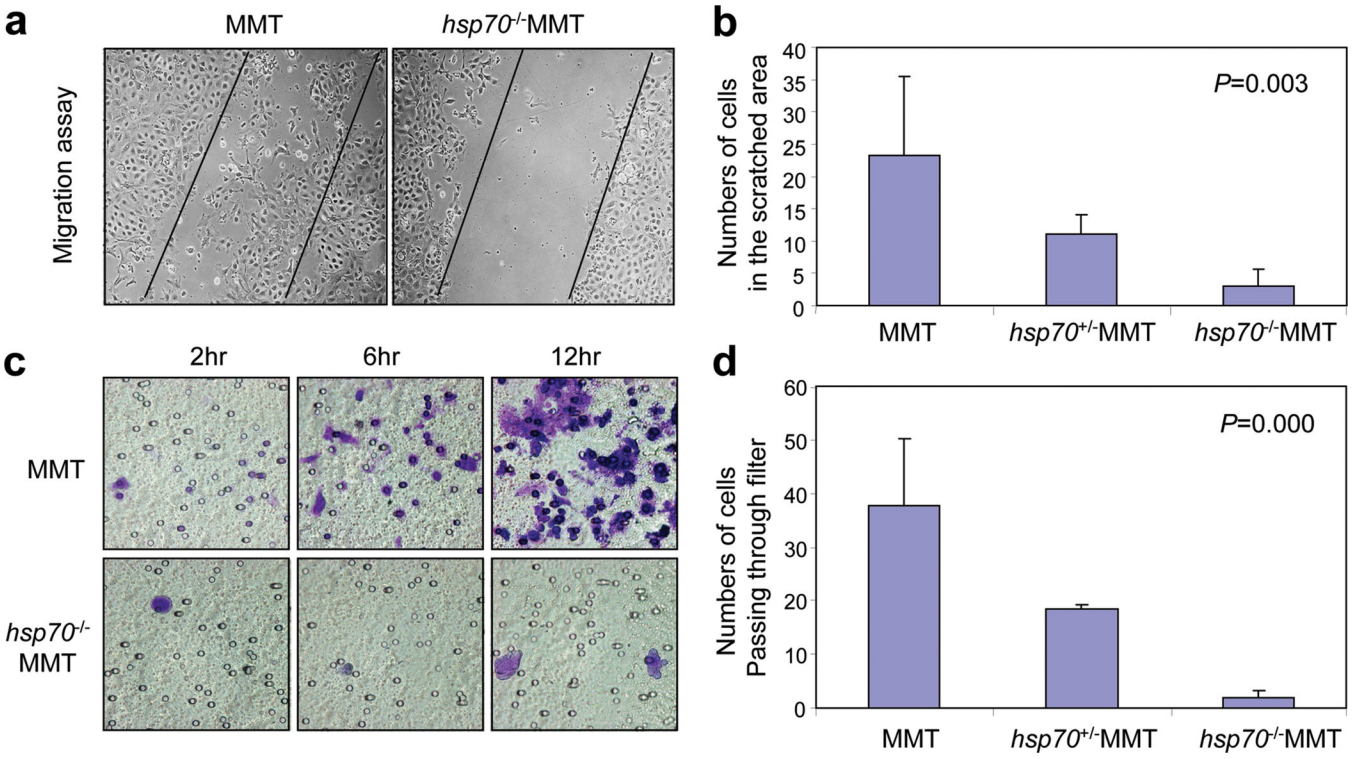

Figure 5. Reduced migration ability of tumor cells without *hsp70*.

(**a and b**) Wound healing assay. Mammary tumor cells were cultured and the cell monolayer was scratched by scalpel. The cells migrating to the scratched areas were then counted and assessed numbers were presented in the bar graph. (**c and d**) Two chamber migration assay. Mammary tumor cells were isolated from MMT and *hsp70*$^{-/-}$MMT mice and cultured. The cells were then placed on the upper well of the chamber separated by the filter and cultured. The filters were removed at indicated times and the cells passing through the filter (lower side of the filter) were fixed and stained with 0.5% Crystal violet. The cells were counted under microscopy (40x) and presented in bar graph. (**b and d**) The results were summary of three experiments. The error bars indicated standard deviation. *P* values were obtained by *one-way ANOVA*.

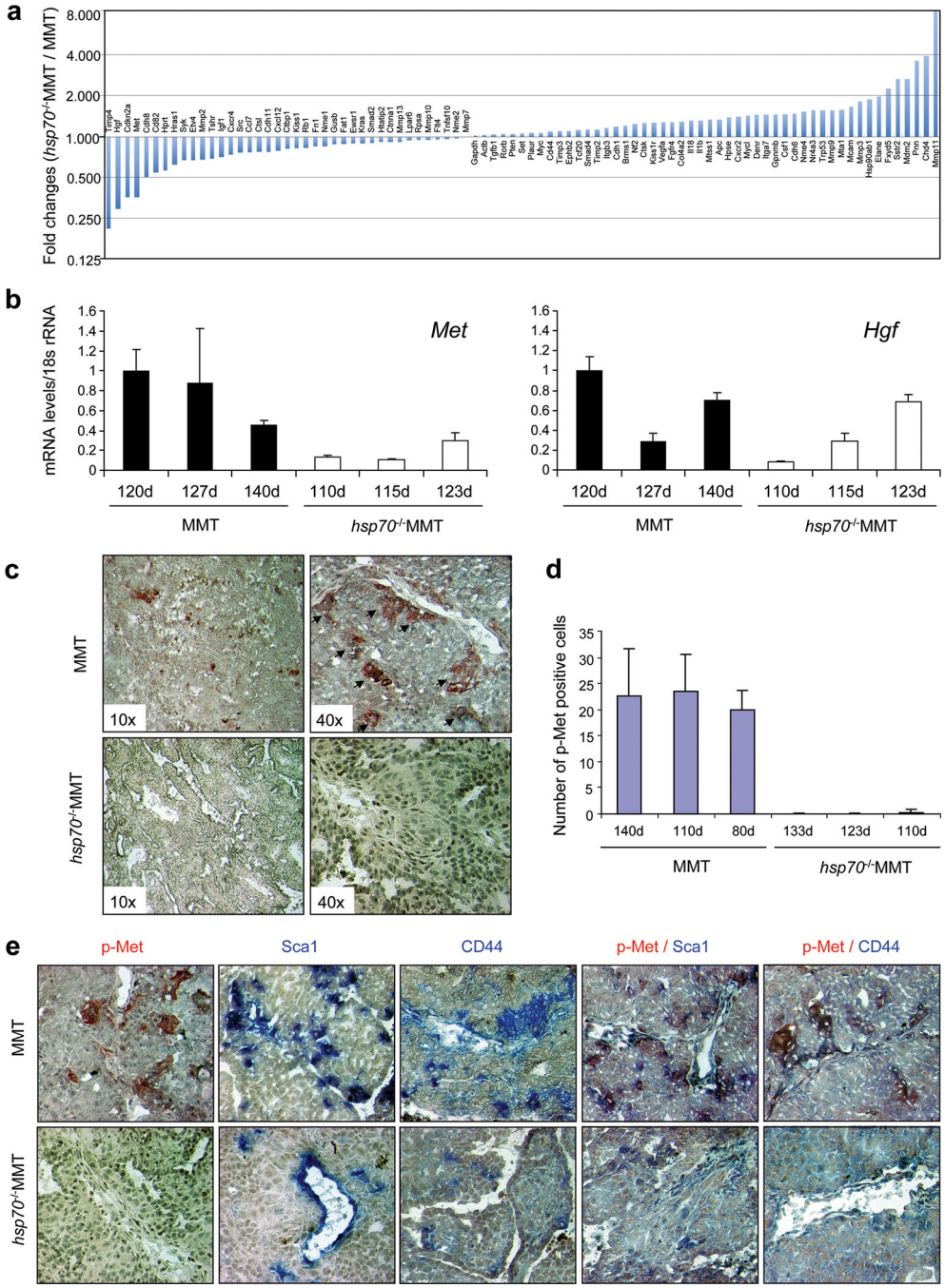

Figure 6. Gene expression profiling of tumors from MMT and *hsp70*$^{-/-}$MMT mice by RT^2 qPCR array, the expression of *Met* and *Hgf* by qRT-PCR and analysis of intratumor phospho-Met distribution by immunohistochemical staining.

(a) The fold changes in mRNAs extracted from MMT (134 and 140 days old) and *hsp70*$^{-/-}$MMT (134 and 133 days old) tumors detected by the RT^2-qPCR array for metastasis-associated transcripts. (**b**) Comparison of *Met* and *Hgf* expression in tumors from MMT and *hsp70*$^{-/-}$MMT mice by qRT-PCR. Total RNAs were purified from tumor tissues obtained from MMT and *hsp70*$^{-/-}$MMT mice. Expression of *Met, Hgf* and 18s rRNA were quantified by qRT-PCR. Values were normalized to 18s rRNA level. Each tumor sample was

performed in duplicate and experiments repeated three times. Error bars indicate standard deviation. $P<0.05$ in *Met* expression was obtained using Student's *t*-test. (**c**) p-Met levels in tumors from MMT and *hsp70*$^{-/-}$MMT mice. Tumors from MMT and *hsp70*$^{-/-}$MMT mice were sectioned after freezing and stained red with mAb against phosphorylated c-Met (Y1349). Arrows indicate the p-Met positive cells. (**d**) Quantitation of p-Met staining. The p-Met positive cells were counted in ten randomly selected fields for each mouse at 40× magnifications. The averages of positive cells per field in individual mice were presented in the bar graph. The error bars indicated standard deviation. (**e**) Detection of the cells co-expressing stem cell markers and p-Met. Tumors from MMT and *hsp70*$^{-/-}$MMT mice were sectioned after freezing and stained with mAbs against phosphorylated c-Met (Y1349) (red color) and/or Sca1 (blue color) or CD44 (blue color). The double positive cells were stained purple and the photographs were 40x magnification.

Table 1

Numbers of tumor colonies in lungs

Mouse	Age (Days)	Numbers of Tumor Colonies*	Average ± SD
MMT	112	17	11.2 ± 4.97
MMT	120	6	
MMT	127	13	
MMT	140	6	
MMT	140	14	
hsp70$^{-/-}$MMT	115	0	0 ± 0.00
hsp70$^{-/-}$MMT	124	0	
hsp70$^{-/-}$MMT	124	0	
hsp70$^{-/-}$MMT	124	0	
hsp70$^{-/-}$MMT	147	0	

*Lungs from each mouse were embedded and total 10 sections (5μm) were randomly obtained from each block with at least 10 sections interval between sections. The sections were stained with hematoxylin and eosin (H&E). The microscopic tumor nodules were counted under a light microscope and summarized in the Table with average and standard deviation. *T-test* was used for statistical analysis (p=0.007). It should be noted that large tumors in MMT mice can be presented in multiple sections and counted as a microscopic tumor nodule in each section.

Table 2

Top20 genes increased or decreased by *hsp70* knockout

	Decreased			Increased	
	Gene	**Fold Change**		**Gene**	**Fold Change**
1	Timp4	0.22	1	Mmp11	8.03
2	Hgf	0.31	2	Chd4	3.81
3	Cdkn2a	0.37	3	Pnn	3.51
4	Met	0.37	4	Mdm2	2.59
5	Cdh8	0.52	5	Sstr2	2.58
6	Cd82	0.56	6	Fxyd5	2.22
7	Hprt	0.57	7	Elane	1.95
8	Hras1	0.63	8	Hsp90ab1	1.86
9	Syk	0.68	9	Mmp3	1.80
10	Etv4	0.68	10	Mcam	1.65
11	Mmp2	0.69	11	Mta1	1.56
12	Tshr	0.70	12	Mmp9	1.55
13	Igfr	0.71	13	Trp53	1.55
14	Cxr4	0.75	14	Nr4a3	1.55
15	Src	0.77	15	Nme4	1.51
16	Ccl7	0.77	16	Cdh6	1.46
17	Ctsl	0.79	17	Csf1	1.45
18	Cdh11	0.79	18	Gpnmb	1.45
19	Cxcl12	0.80	19	Itga7	1.45
20	Ctbp1	0.82	20	Denr	1.44